

INWARD MOTIONS IN STARLESS CORES TRACED WITH CS (3-2) and (2-1) LINES

CHANG WON LEE^{1,2}, PHILIP C. MYERS², AND RENÉ PLUME^{2,3}

¹Korea Astronomy Observatory, 61-1 Hwaam-dong, Yusung-gu, Daejeon 305-348, Korea

E-mail: cwl@trao.re.kr

²Harvard-Smithsonian Center for Astrophysics, 60 Garden Street, MS 42, Cambridge, MA 02138, USA

³University of Calgary, Department of Physics & Astronomy, 2500 University Drive NW, Calgary, Alberta, Canada T2N 1N4

(Received August 1, 2004; Accepted December 13, 2004)

ABSTRACT

We compare the results of the surveys of starless cores performed with CS (2-1) and (3-2) lines to study inward motions in the cores. The velocity shifts of the CS(3-2) and (2-1) lines with respect to N_2H^+ are found to correlate well with each other and to have similar number distributions, implying that, in many cores, systematic inward motions of gaseous material may occur over a range of density of at least a factor ~ 4 . Fits of the CS spectra to a 2-layer radiative transfer model in ten infall candidates suggest that the median effective line-of-sight speed of the inward-moving gas is $\sim 0.07 \text{ km s}^{-1}$ for CS (3-2) and $\sim 0.04 \text{ km s}^{-1}$ for CS(2-1). Considering that the optical depth obtained from the fits is usually smaller in CS(3-2) than in (2-1) line, this may indicate that CS(3-2) usually traces inner, denser gas with greater inward motions than CS(2-1) implying that many of the infall candidates have faster infall toward the center. However, this conclusion may not be representative of all starless core infall candidates, due to the statistically small number analyzed here. Further line observations will be useful to test this conclusion.

Key words : ISM: Globules; ISM: Kinematics and Dynamics; Stars: Formation

I. INTRODUCTION

The inward motions in starless cores, dense ($\gtrsim 10^4 \text{ cm}^{-3}$) condensations without any embedded YSOs in molecular clouds, are one of the essential elements needed to understand the initial onset of star formation. These motions can be studied by detecting the spectral “*infall asymmetry*” (Hummer & Rybicki 1968; Leung & Brown 1977; Lee, Myers, & Tafalla 1999-hereafter LMT99). Two molecular lines CS(3-2) and CS(2-1) are known to be good tracers of inward motions because they often show such an infall asymmetry useful to study inward motions in starless cores. The CS(3-2) line has higher critical density ($n_{\text{cr}} \approx 1.3 \times 10^6 \text{ cm}^{-3}$) than CS(2-1) by a factor of about 4 (Evans 1999) and thus, the CS(3-2) line will be a better probe of the kinematics closer to the nucleus of the core unless the optical depth of the CS(3-2) is larger than CS(2-1). Hence, both CS lines are useful tracers of inward motions over a density range of at least a factor of ~ 4 in the core. In this paper we compare CS(3-2) and (2-1) spectra to discuss how inward motions in starless cores occur. More details on this study can be found in Lee, Myers, & Plume (2004; hereafter LMP04).

II. DATA

Details about the surveys of starless cores with CS(3-2) and (2-1) transitions are described in LMT99 and LMP04. These two surveys produced data sets of CS(2-1), (3-2) and N_2H^+ (1-0) lines for ~ 70 starless cores. They provide a fairly good-sized sample to statistically study inward motions by comparing velocity shifts of the skewed CS spectra with respect to the velocity of the optically thin tracer (N_2H^+ 1-0 in this case). We also apply a two layer radiative transfer model to the spectra.

III. δV ANALYSIS FOR CS(3-2) AND (2-1)

The degree of spectral asymmetry in the CS profiles is quantitatively measured by the normalized velocity difference [$\delta V_{\text{CS}} = (V_{\text{CS}} - V_{N_2H^+})/\Delta V_{N_2H^+}$] between CS(3-2) or (2-1), and N_2H^+ (1-0) (Mardones et al. 1997). V_{CS} is the velocity determined from a Gaussian fit to the brighter spectral component of the CS(3-2) or (2-1) profile. $V_{N_2H^+}$ and $\Delta V_{N_2H^+}$ are the velocity and FWHM of N_2H^+ (1-0) taken from LMT99.

Fig. 1 compares the distribution of $\delta V_{\text{CS}32}$ with that of $\delta V_{\text{CS}21}$ from LMT99 for a sample of over 65 starless cores, showing that both $\delta V_{\text{CS}32}$ and $\delta V_{\text{CS}21}$ distributions are similarly skewed to the blue side ($\delta V_{\text{CS}} < 0$). In addition, the average (\pm s.e.m – standard error of the mean of the distribution) of $\delta V_{\text{CS}32}$ is -0.14 ± 0.03 which is also similar to the average

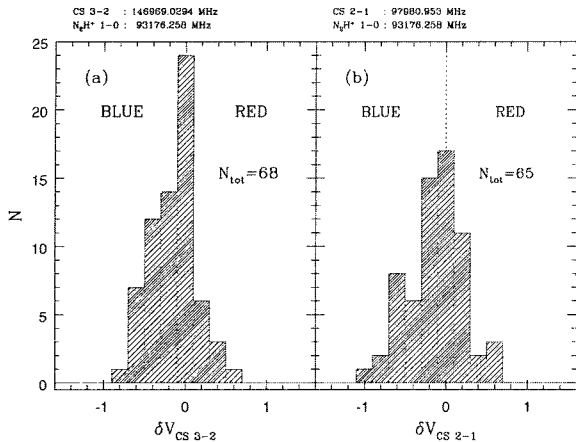


Fig. 1.— Histograms of the normalized velocity differences between CS(3-2) and N_2H^+ 1-0, and CS(2-1) and N_2H^+ 1-0.

of δV_{CS21} (-0.13 ± 0.04). Given the expectation that CS(3-2) is a better probe of the denser inner region, one might expect a more skewed δV distribution for CS(3-2) than for CS(2-1). However, the δV distribution for CS(3-2) is found to be statistically very similar to that for CS(2-1). What does this imply about inward motions in cores? We see in the following section §V that CS(3-2) traces faster infalling gas than does CS(2-1) by typically $\sim 0.03 \text{ km s}^{-1}$. The increase in infall velocity would result in a similar increase in line velocity which was used to compute δV . Note, however, that this increase is not that great compared to the N_2H^+ line width, typically 0.3 km s^{-1} . Therefore the typical increase in δV is about $0.03/0.3$, or 0.1, or only about half of a bin size in the histograms of Fig. 1 which explains why the histograms look similar despite the higher critical density and higher infall speed for CS(3-2) compared to (2-1). The similar δV distribution between CS(3-2) and CS(2-1) may suggest that, in many cores, inward-moving gas extends over a substantial range of core densities.

Fig. 2 compares the δV 's of CS(3-2) with those of CS(2-1) for each source, showing a good correlation (correlation coefficient, $r = 0.79$) between the two transitions. This may suggest that the lower density and higher density gas probed by the 2-1 and 3-2 lines, respectively, move together in a systematic rather than random fashion.

IV. SELECTION OF INFALL CANDIDATES

Infall candidates are chosen to study their inward motions. With more molecular line data we can better identify infall candidates. Therefore, we combine the CS(3-2) and DCO^+ data from LMP04 with the CS(2-1) and N_2H^+ data of LMT99. To identify infall candidates we use the following properties of the spec-

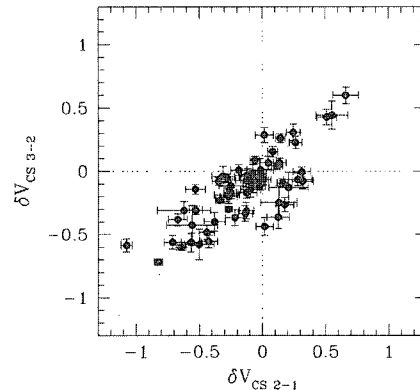


Fig. 2.— Correlation between the normalized velocity differences of CS(3-2) and CS(2-1) for all sources.

tra from LMT99 and LMP04; (1) the values of δV for CS(2-1), CS(3-2), and $DCO^+(2-1)$ with respect to the $N_2H^+(1-0)$, (2) the intensity ratios (T_b/T_r) of the blue to red components in double-peaked CS and DCO^+ spectra, and the main component in N_2H^+ spectra. These properties are flagged by “color codes”: 1 for $\delta V \leq -5\sigma_{\delta V}$ (a blue normalized velocity difference), 0 for $|\delta V| < 5\sigma_{\delta V}$ (neutral), and -1 for $\delta V \geq 5\sigma_{\delta V}$ (a red normalized velocity difference). Property (2) is indicated by a 1 for $T_b/T_r > 1 + \sigma$ (blue peak stronger than the red peak), 0 for $1 - \sigma \leq T_b/T_r \leq 1 + \sigma$ (peaks of equal strength), and -1 for $T_b/T_r < 1 - \sigma$ (red peak stronger than the blue peak), where the values of T_b and T_r were derived from Gaussian fits to each component of the spectra with double peaks (or single peak with a distinct shoulder).

Using the statistics of the color codes, we define *strong infall candidates* if each shows at least four indications of infall asymmetry and no counter-indications in the sense that nearly all their spectral properties are given ‘blue’ flags. Such sources are **L1355**, **L1498**, **L1521F**, **L1544**, **L158**, **L492**, **L694-2**, and **L1155C-1**.

V. INFALL SPEEDS DERIVED FROM CS SPECTRA AND THEIR IMPLICATION

Infall speeds are derived for a sub-sample of cores via fits to their CS spectra using a two-layer model consisting of a cool (2.7 K) absorbing front screen moving away from us and a warm emitting rear layer approaching us with the same speed (see Lee, Myers, & Tafalla 2001). Fits were conducted for the CS(3-2) profiles of 12 sources showing the infall asymmetry.

Fig. 3 shows that our model easily reproduces the observed spectral features. Typical 1-D infall speeds for the sources modeled are $\sim 0.02 - 0.13 \text{ km s}^{-1}$. We also obtained the infall speeds for a sub-sample of 8

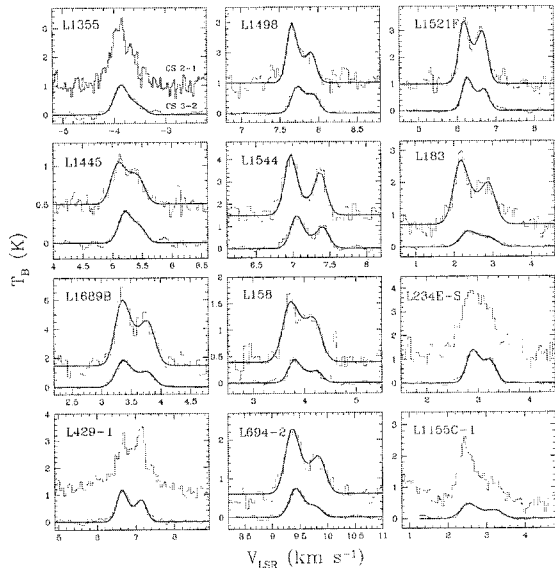


Fig. 3.— Two-layer radiative transfer model fits to CS spectra in twelve infall candidates. Twelve sources for which the CS(3-2) or (2-1) profiles show infall asymmetry were chosen because their spectra have either double peaks or a blue peak with a clear red shoulder. These types of spectra allow us to accurately determine the infall speeds with small uncertainties.

sources using fits to the CS(2-1) spectra which show similar asymmetry to that of CS(3-2). The resulting infall speeds derived from our model fits to both the CS(3-2) and CS(2-1) observations are compared in Fig. 4. A noticeable feature in Fig. 4 is that the CS(3-2) lines generally have higher infall speeds than CS(2-1); typically $\sim 0.07 \text{ km s}^{-1}$ for CS (3-2) and $\sim 0.04 \text{ km s}^{-1}$ for CS (2-1).

The difference between two infall speeds measured from CS(3-2) and (2-1) lines is found to be significantly larger than any possible errors produced in determining infall speeds from several tests (see LMP04 for details). Considering that the CS(3-2) lines have lower optical depth than CS(2-1) lines for all sources except for L158 and L1445 (see Table 3 in LMP04), we conclude that CS(3-2) traces faster, inner gas than does CS(2-1). However, we are still cautious of whether this is necessarily true of most starless cores, or even of most infall candidates, because of the small number of objects involved in our analysis. Further detailed observations of more infall candidates with the same lines are needed to test whether the conclusion generally apply to starless cores or most infall candidates.

ACKNOWLEDGEMENTS

C.W.L. greatly acknowledges supports from the Basic Research Program (KOSEF R01-2003-000-10513-0)

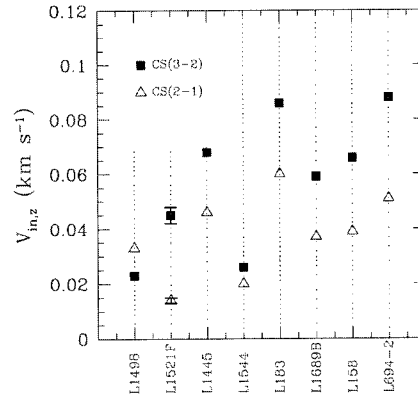


Fig. 4.— Infall speeds derived from our two layer model fits to CS(2-1) and CS(3-2) profiles. The error bars for L1521F represent 1 sigma uncertainties of the distribution of infall speeds obtained from repeated fits of two-layer models to each twenty synthetic CS(2-1) and (3-2) spectra (see LMP04 for details).

of the Korea Science and Engineering Foundation, and Strategic National R&D Program (M1-0222-00-0005) from Ministry of Science and Technology, Republic of Korea.

REFERENCES

- Evans, N. J. 1999, ARAA, 37, 311
- Hummer, D., & Rybicki, G.B. 1968, ApJ, 153, 107
- Lee, C. W., Myers, P.C., & Tafalla, M. 1999, ApJ, 526, 788 (LMT99)
- Lee, C. W., Myers, P.C., & Tafalla, M. 2001, ApJS, 136, 703
- Lee, C. W., Myers, P.C., & Plume, R. 2004, ApJS, 153, 523 (LMP04)
- Leung, C.M., & Brown, R.B. 1977, ApJ, 214, L73
- Mardones, D., Myers, P.C., Tafalla, M., Wilner, D.J., Bachiller, R., & Garay, G. 1997, ApJ, 489, 71